Asian Journal of Chemistry; Vol. 25, No. 6 (2013), 3187-3194

ASIAN JOURNAL OF CHEMISTRY

http://dx.doi.org/10.14233/ajchem.2013.13588

Hydrogen Production from Methanol Steam Reforming over $Ce_{0.9}Cu_{0.1}O_Y$ Solid Solution Catalysts: The Effect of Preparation Methods

LIRONG ZHANG[1], YUHONG WANG[2,*], JUN YU[2], ROGER WHITING[3] and FENGPING YI[1]

[1]School of Perfume and Aroma Technology, Shanghai Institute of Technology, Shanghai 201418, P.R. China
[2]Research Institute of Applied Catalysis, School of Chemical and Environmental Engineering, Shanghai Institute of Technology, Shanghai 201418, P.R. China
[3]School of Applied Science, Faculty of Health and Environmental Sciences, Auckland University of Technology, Auckland, New Zealand

*Corresponding author: Tel: +86 21 60873558; E-mail: yuhong_wang502@hotmail.com

(*Received*: 13 February 2012; *Accepted*: 14 December 2012) AJC-12545

A series of $Ce_{0.9}Cu_{0.1}O_Y$ catalysts were prepared using various methods including deposition-precipitation, conventional aqueous coprecipitation and sol-gel precipitation. The physical and chemical properties of the prepared catalysts were characterized using TEM, Raman, UV-VIS, XRD, H_2-TPR and XPS techniques. These indicate that a solid solution was formed in the product. Steam reforming of methanol was carried out over $Ce_{0.9}Cu_{0.1}O_Y$ catalysts and showed moderate methanol conversion and high selectivity to H_2 and CO_2. The investigation indicates that the preparative method significantly affects the active species dispersion, microstructure and the resulting catalytic performance with respect to conversion and selectivity. The $Ce_{0.9}Cu_{0.1}O_Y$ catalyst prepared by a deposition-precipitation method displayed higher specific surface area, greater reductive ability and higher activity for methanol conversion as compared to the catalysts prepared by other methods.

Key Words: Solid solution, $Ce_{0.9}Cu_{0.1}O_Y$, Methanol steam reforming, Hydrogen production, Preparation method.

INTRODUCTION

Hydrogen is considered as an ideal source of clean energy and a number of major energy companies have become increasingly prominent in its development. However it has drawbacks in terms of sourcing, storage and transport which have impeded its wide application[1]. Methanol can be converted to hydrogen by three methods including partial oxidation, decomposition and the steam reforming. Among these, partial oxidation and steam reforming might considered be more attractive to methods to produce hydrogen. Nevertheless the methanol steam reforming process has advantages of low cost, mild conditions, low CO content and a product easily separated to provide hydrogen[2-4].

Recently much attention has been paid to the studies on catalysts with stability and high catalytic activities at low reaction temperatures for hydrogen production by steam reforming of methanol. A large variety of catalytic materials for the steam reforming of methanol (SRM) reaction, including Ni[5-7], Pd[8-11] and Cu[12-16] based catalysts, have been reported in the literature. In comparison, low cost and high activity makes Cu based catalysts widely applied and investigated for the steam reforming of methanol. Kobayashi *et al.*[17] studied the effect of supports and demonstrated that catalysts using Al_2O_3 or ZrO_2 as support gave high catalytic activity. The catalytic activity and stability of Au-Cu-Fe quasicrystal (QC) and crystalline alloy catalysts prepared by alkali leaching for steam reforming of methanol were tested and demonstrated that the QC catalyst showed a higher catalytic activity and stability than the crystalline ones[18]. Additionally, steam reforming and oxidative steam reforming of methanol were carried out over a series of coprecipitated CuO-CeO_2 catalysts with varying copper content which exhibited satisfactory activity in low reaction temperature[19].

The use of CeO_2-based catalysts has shown a rapid increase in the recent years[20]. The high oxygen mobility[21] and strong metal-support interaction[22] render the CeO_2-based materials very interesting both as a catalyst and as a support. It is well known that ceria is not just an inert for supported species, but also a modifier affecting the degree of dispersion as well as the redox behaviour and catalytic activity of supported catalysts[23]. The incorporation of metal ions into the CeO_2 lattice forms $Ce_{1-X}M_XO_Y$ solid solutions, which can give the better redox properties than those of pure CeO_2[24-28]. Much research relating to Cu-Ce-O analogue catalysts has focused on the applications to the selective oxidation of CO in excess

hydrogen at low temperatures[29-31]. Furthermore, Ce-Cu-O solid solutions showed high catalytic activity and selectivity in the oxidative steam reforming of methanol (OSRM). Shan *et al*. investigated oxidative steam reforming of methanol reaction over $Ce_{0.9}Cu_{0.1}O_Y$ solid solution catalyst prepared by complexation-combustion method. High activity and selectivity was obtained, in addition the characterizations suggested that the catalytic activity is related to the solid solution structure and the higher redox properties[27].

Only few investigations have been carried out on hydrogen production from the steam reforming of methanol reaction over Ce-Cu-O solid solution catalysts[27,32]. Consideration of the higher redox properties and higher activity of Cu-based catalysts for steam reforming of methanol suggests that, a high catalytic activity could be expected for steam reforming of methanol over Ce-Cu-O solid solution catalysts. Liu *et al.*[32] reported the synthesis of $Ce_{1-x}Cu_xO_{2-x}$ mixed oxides by coprecipitation. These mixed oxides partly formed solid solutions when $x < 0.2$. All the Cu-containing catalysts tested in the steam reforming of methanol exhibited high selectivity to CO_2 and H_2 and relatively high conversions[33].

It has been widely accepted that catalytic performance of an inorganic material catalyst is greatly related to its method of preparation which always has effect on the structural characteristics of the catalyst. Herein, we investigated and compared the effect of the preparation method of $Ce_{0.9}Cu_{0.1}O_Y$ solid solution on the catalytic activity toward the steam reforming of methanol reaction.

This paper reports the preparation of a series of $Ce_{0.9}Cu_{0.1}O_Y$ catalysts by different methods including coprecipitation, deposition-precipitation and the sol-gel method as well as their performance in the steam reforming of methanol reaction. The preparation methods affected the microstructure, reducibility and catalytic activity of solid solutions. It was found that the $Ce_{0.9}Cu_{0.1}O_Y$ prepared by deposition-precipitation method showed high catalytic activity. In addition, the effect of methanol flow rate and water/methanol ratio was investigated.

EXPERIMENTAL

Three $Ce_{0.9}Cu_{0.1}O_Y$ catalysts with a Ce/Cu atom mole ratio of 9/1 were prepared by different methods.

Deposition precipitation: The sample $Ce_{0.9}Cu_{0.1}O_Y$-dp was prepared by the deposition-precipitation method. CeO_2, was used as a support for the catalyst, was prepared by the precipitation of aqueous solution $Ce(NO_3)_3{\cdot}6H_2O$ with addition of $NaHCO_3$ (0.15 M) at 70 ºC until pH reached 8.0. The precipitant was left in the mother liquor for 2 h, followed by filtration and washing with deionized water. The solid formed was dried at 100 ºC overnight and calcined at 450 ºC for 5 h. Then the CeO_2 support was suspended in an aqueous solution containing an appropriated amount of $Cu(NO_3)_2{\cdot}3H_2O$. An aqueous solution of $NaHCO_3$ (0.15 M) was gradually added to the suspension with stirring at 70 ºC until the pH of the mixed solution reached 8. The precipitate which formed was left for 2 h at the same temperature, then filtered, washed and dried overnight at 100 ºC. The precursor was calcined at 450 ºC for 5 h.

Co-precipitation: The catalyst $Ce_{0.9}Cu_{0.1}O_Y$-cp was prepared by the conventional co-precipitation method. The aqueous solution of $Cu(NO_3)_2{\cdot}3H_2O$ and $Ce(NO_3)_3{\cdot}6H_2O$ coprecipitated at 70 ºC using $NaHCO_3$ (0.15 M) as the precipitating agent. The pH was kept constant at 7.5-8.0. After being aged at 70 ºC for 2 h under vigorous stirring, the precipitate was filtered and washed with deionized water thoroughly, dried at 100 ºC overnight and finally calcined at 450 ºC for 5 h.

Sol-gel method: The catalyst $Ce_{0.9}Cu_{0.1}O_Y$-sg was prepared by sol-gel method as described below. An aqueous solution of 20 % excess of oxalic acid is added into the mixed solution of $Cu(NO_3)_2{\cdot}3H_2O$ and $Ce(NO_3)_3{\cdot}6H_2O$ at 70 ºC with vigorous stirring. The gel formed was dried at 110 ºC to remove the solvents and then calcined at 450 ºC for 5 h to give the desired precursor.

Catalyst characterization: The surface areas and pore size distribution of the samples were calculated by nitrogen adsorption-desorption method recorded on a Micrometric ASAP2020 instrument. High-resolution transmission electron microscope characterization was performed with a JEM-2100 operated at 200 kV. The X-ray powder diffraction (XRD) analysis was performed using a D/Max-2000 X-ray diffractometer with CuK_α radiation. The working voltage and current of the X-ray tube were 40 kV and 100 mA. Fourier transform Raman spectra were recorded with Dilor LabRam-1B Raman spectrometer. The UV-VIS spectra of the samples were performed with a CARY1000Bio UV-VIS spectrophotometer using a quartz cell. X-Ray photoelectron spectra (XPS) were performed with a Kratos Axis Ultra DLD equipped with a AlK_α radiation of exciting photoelectrons. Temperature-programmed reduction (TPR) experiments were carried out in a continuous flow fixed-bed reactor under the mixture of 10 % H_2 in N_2 flowing (30 mL min^{-1}) over 50 mg catalyst at a heating rate of 10 ºC/min. The amount of H_2 consumed was monitored with a TCD detector.

Catalyst activity measurements: Catalyst samples activity were tested using a continuous flow fixed-bed microreactor at atmospheric pressure. A 0.3 g sample of the catalyst was diluted with 1.0 g quartz sand and packed in a tubular reactor and then pre-reduced in a H_2 flowing at 300 ºC for 2 h. Mixtures of water and methanol with a known molar ratio were evaporated and delivered into the catalytic reactor *via* a heated gas feeding system. The gaseous products which including H_2, CO, CO_2, CH_4 were detected on-line by the FULI9790AGC-MS instrument to determine their compositions.

RESULTS AND DISCUSSION

Characterization of the $Ce_{0.9}Cu_{0.1}O_Y$ catalysts: Fig. 1 shows the TEM micrographs of the three $Ce_{0.9}Cu_{0.1}O_Y$ catalysts prepared by different methods. In all cases it can be observed that the morphology of the catalysts depended on the preparation routes, although copper particles could not be distinguished from cerium. The $Ce_{0.9}Cu_{0.1}O_Y$-dp sample obtained by deposition-precipitation afforded agglomerates much larger than those of the other samples. The image of $Ce_{0.9}Cu_{0.1}O_Y$-cp reveals a rather foamlike structure resulting from closely aggregated metal oxide nanoparticles[33]. The particles composing the catalyst $Ce_{0.9}Cu_{0.1}O_Y$-sg show mostly regular spherical shapes and the distribution of the main active particles seems to be practically uniform. In addition, the TEM image of $Ce_{0.9}Cu_{0.1}O_Y$-sg shows obviously larger particle sizes than were

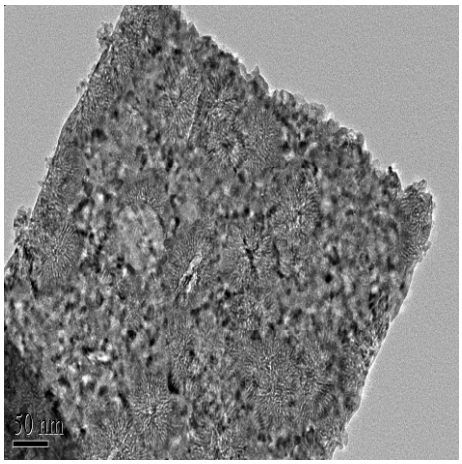

(a)

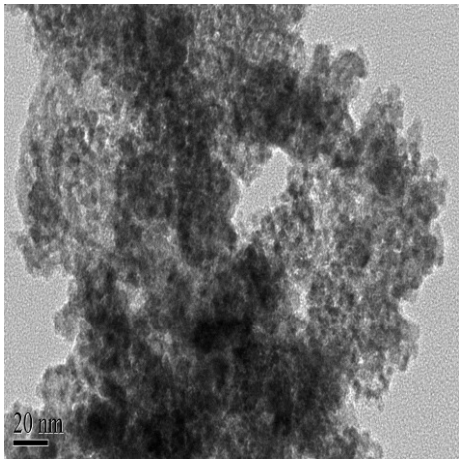

(b)

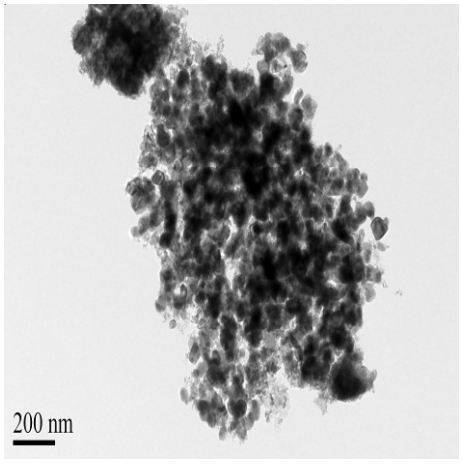

(c)

Fig. 1. TEM micrographs (a) $Ce_{0.9}Cu_{0.1}O_Y$-dp; (b) $Ce_{0.9}Cu_{0.1}O_Y$-cp; (c) $Ce_{0.9}Cu_{0.1}O_Y$-sg

present in the images of $Ce_{0.9}Cu_{0.1}O_Y$-dp and $Ce_{0.9}Cu_{0.1}O_Y$-cp. On the other hand, it is supposed, from the image presented, that the CeO_2 crystallites are enveloped by either amorphous foam or very small clusters of CuO. Indeed, the lower scattering power of copper compared to that of cerium cannot favour the commonly higher metal density of active phase of a catalyst than the support[34].

The measured data of the BET surface areas, pore volumes and pore sizes of the $Ce_{0.9}Cu_{0.1}O_Y$ catalysts prepared by various methods are listed in Table-1. The $Ce_{0.9}Cu_{0.1}O_Y$-dp has a similar BET surface area to that of $Ce_{0.9}Cu_{0.1}O_Y$-cp and its pore volume is much higher than that of other two samples. It is noted that the BET surface area of $Ce_{0.9}Cu_{0.1}O_Y$-dp sample is very close to the CuO/CeO_2 materials prepared with aqueous ammonia solution as precipitating agent as reported by Tang *et al.*[35]. While the $Ce_{0.9}Cu_{0.1}O_Y$-sg sample shows a largest particle size compared with the others. The results indicate that the preparation method affected the physical properties of the catalyst particles such as particle size and morphology, which are of critical importance for its applications in catalysis[36].

TABLE-1
BET SURFACE AREA, PORE VOLUME, PORE SIZE AND LATTICE PARAMETER OF THE $Ce_{0.9}Cu_{0.1}O_Y$ CATALYSTS

Sample	BET (m^2/g)	Pore volume ($mL/g \times 10^{-2}$)	Particle size (nm)	Lattice parameter (Å)
$Ce_{0.9}Cu_{0.1}O_Y$-dp	93.0	8.3	6.8	5.4030
$Ce_{0.9}Cu_{0.1}O_Y$-cp	96.7	6.9	5.9	5.4050
$Ce_{0.9}Cu_{0.1}O_Y$-sg	85.3	7.5	10.5	5.4040

The XRD patterns of the prepared $Ce_{0.9}Cu_{0.1}O_Y$-dp, $Ce_{0.9}Cu_{0.1}O_Y$-cp and $Ce_{0.9}Cu_{0.1}O_Y$-sg catalysts are shown in Fig. 2. The distinct CeO_2 fluorite-type oxide structure was present in all samples. Furthermore, when the calcining temperature increased to 850 ºC, it had obvious effect on the broadenings and relative peak intensities of CeO_2 phase. It indicates that only high temperature treatment affects the degree of crystallinity and the particle size of the CeO_2 phase. However, XRD showed no obvious lines of CuO diffraction peaks even when the heating temperature increased to 850 ºC. This may be attributed to the formation of an amorphous phase, a fine dispersion of CuO on the surface of CeO_2, Cu-Ce-O solid solution formation or a combination of these phenomena[37-40]. On the other hand, from a comparison of the diffraction peaks of CeO_2 in these catalysts, one can find the diffraction peaks of $Ce_{0.9}Cu_{0.1}O_Y$-dp and $Ce_{0.9}Cu_{0.1}O_Y$-sg are shifted towards lower 2θ values compared to those of $Ce_{0.9}Cu_{0.1}O_Y$-cp catalysts. This noticeable shift could be ascribed to the lattice expansion (Table-1). Oxygen released from CeO_2 with the increase in temperature has also been observed and resulted in the formation of CeO_{2-x} species with oxygen vacancies. These could cause lattice expansion[41]. Therefore, the presence of Ce^{3+} ions from partial reduction of Ce^{4+} gave rise to the peak shift and particle expansion (radius Ce^{4+} = 0.92 Å and radius Ce^{3+} = 1.03 Å). Compared with CeO_2 (5.4120 Å), the cell parameters of $Ce_{0.9}Cu_{0.1}O_Y$ were slightly smaller, because when part of the CuO incorporates into the CeO_2 lattice and replace Ce^{4+}, a reduction of the cell parameter of ceria occurs. Hence, the formation of oxygen vacancies was expected to be responsible for the lattice expansion, which might be due to the defects in solid solution structure. The diffraction peak shift and change of cell parameters suggested that the formation of a solid solution might be responsible for the absence of CuO species in the XRD at low CuO content.

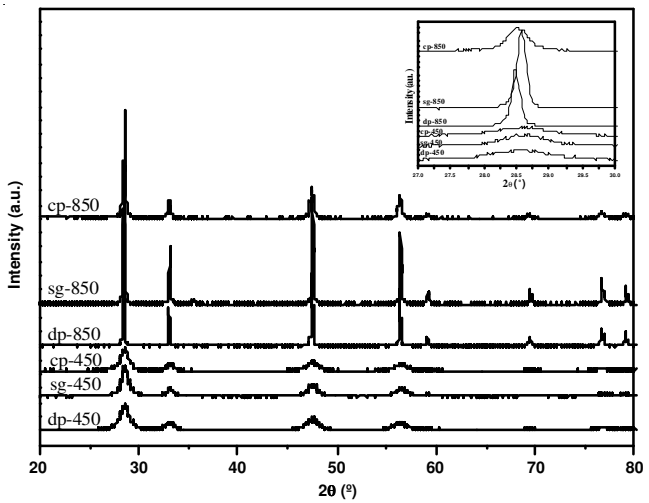

Fig. 2. XRD patterns of the $Ce_{0.9}Cu_{0.1}O_Y$ catalysts prepared with various methods and calcined at 450 and 850 ºC, respectively

The FT-Raman spectra of the catalysts and pure CeO_2 which was calcined at 450 ºC are shown in Fig. 3. CeO_2 has characterized by the strong feature at 461 cm^{-1}, the typical band of a fluorite structural material. For the supported catalysts prepared, no new band appeared and this was consistent with the XRD analytic results. On the other hand, the broader and weaker bands and peak shift to about 445 cm^{-1} were observed for the $Ce_{0.9}Cu_{0.1}O_Y$ catalysts prepared by various methods. Although the changing lattice parameters with the different CeO_2 particle sizes may result in the Raman feature shift as reported in the literature[42], the possibility of the formation of a solid solution cannot be ruled out. This would result in a change of CeO_2 environment in the presence of copper.

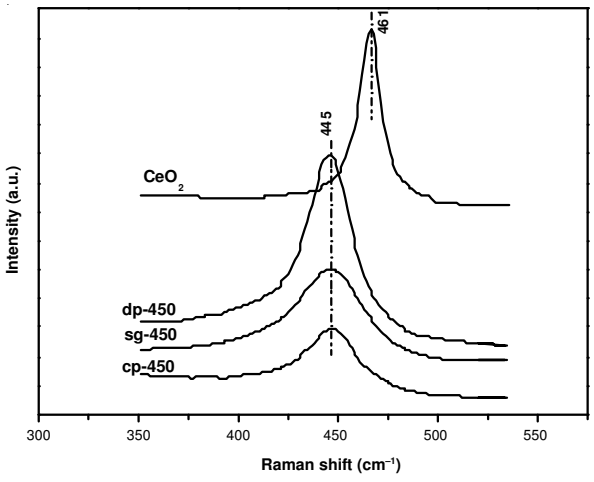

Fig. 3. FT-Raman patterns of CeO_2 and $Ce_{0.9}Cu_{0.1}O_Y$ catalysts

Fig. 4 shows the UV-visible patterns of the prepared $Ce_{0.9}Cu_{0.1}O_Y$ catalysts, CuO, CeO_2 and mixed CuO/CeO_2. The peaks at 258 and 337 cm^{-1} ascribes to the cubic CeO_2 can be observed in samples of CeO_2 and mixed CuO/CeO_2. Comparing with pure CeO_2, it is apparent that the intensity of peak at 337 cm^{-1} decreases and a blue shift occurs for the $Ce_{0.9}Cu_{0.1}O_Y$ samples. The structural defects of CeO_2 with the incorporation of lower valent copper species into the ceria lattice might be responsible to the phenomena.

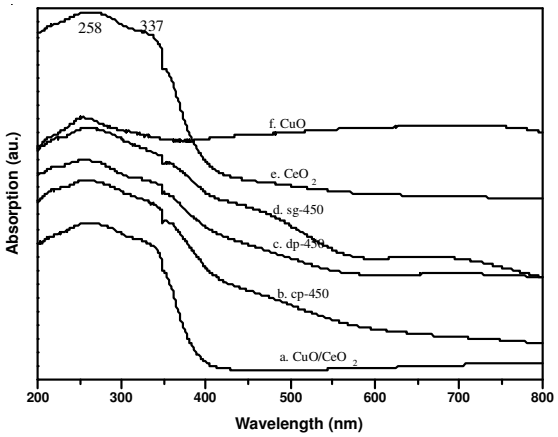

Fig. 4. UV-visible patterns of CeO_2, CuO/CeO_2 and $Ce_{0.9}Cu_{0.1}O_Y$ catalysts

In order to investigate the reducibility of the copper species in the $Ce_{0.9}Cu_{0.1}O_Y$ catalysts prepared by the various methods, temperature programmed reduction (TPR) measurements were performed (Fig. 5). The temperature programmed reduction profile of $Ce_{0.9}Cu_{0.1}O_Y$-dp shows two overlapping reduction peaks at about 209 and 228 ºC. This phenomena is consistent with the reports that CuO supported on CeO_2 showed a two-step reduction at much lower temperatures compared to pure CuO which showed a single reduction at 380-390 ºC[43]. Noticeably, the lower reduction temperature of $Ce_{0.9}Cu_{0.1}O_Y$-dp (*vs*. cp and sg) indicates that the redox properties of CuO are enhanced in the sample prepared by deposition-precipitation method. It is concluded that there is a Cu/Ce interaction which facilitates the reduction of the supported copper species. The temperature programmed reduction peaks at 209 and 228 ºC of $Ce_{0.9}Cu_{0.1}O_Y$-dp may be attributed to reduction of larger CuO particles weakly associated with CeO_2[37,38,44] or CuO micro-clusters in highly dispersed copper oxide materials and the reduction of Cu^{2+} in CeO_2 lattice which would be less reducible than species on the ceria surface[45,46], respectively. The area of peak at 228 ºC is larger than that of peak at 209 ºC also indicating that Cu^{2+} ions in $Cu_xCe_{1-x}O_Y$ solid solution is more difficult to reduce than the copper species dispersed on the support. However, the reduction features of $Ce_{0.9}Cu_{0.1}O_Y$-cp and $Ce_{0.9}Cu_{0.1}O_Y$-sg are different from those of the $Ce_{0.9}Cu_{0.1}O_Y$-dp. The temperature programmed reduction profile of $Ce_{0.9}Cu_{0.1}O_Y$-sg shows three peaks at 279, 303 and 357 ºC, respectively, indicating that the copper oxide species in this sample are more complex than those in dp and cp. The peak at *ca.* 280 ºC in $Ce_{0.9}Cu_{0.1}O_Y$-cp and $Ce_{0.9}Cu_{0.1}O_Y$-sg samples probably represents the reduction of bulk copper oxide (crystalline forms). Interestingly, a peak was observed in the $Ce_{0.9}Cu_{0.1}O_Y$-cp and $Ce_{0.9}Cu_{0.1}O_Y$-sg at *ca.* 358 ºC. One possible explanation is that some of exposed CeO_2 were activated in the course of preparation and reduced at the temperature programmed reduction conditions. The reduced temperature is much lower than that of pure CeO_2 (427 ºC)[35], which suggest that the presence of copper notably promots the reducibility of ceria, especially the surface ceria. Meanwhile, the obvious difference of reducibility of the three samples suggests that there was a big contrast in the degree of solid solution formation. The above discussion demonstrates that the preparation methods exhibited significant effects on the reducibility of the catalysts.

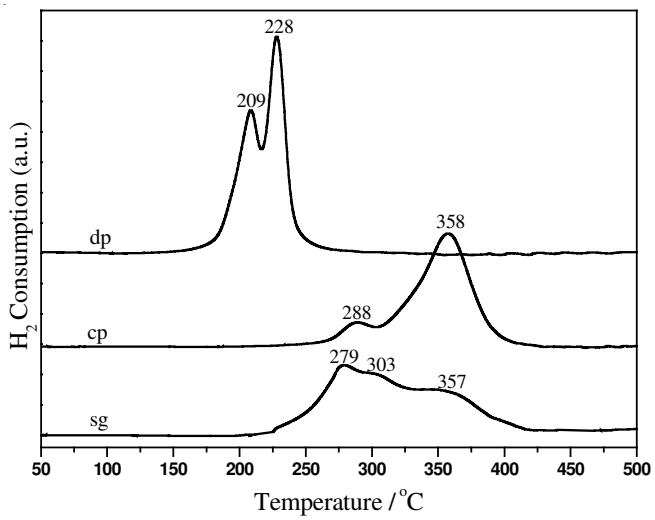

Fig. 5. H_2-TPR profiles of $Ce_{0.9}Cu_{0.1}O_Y$ catalysts prepared by various methods

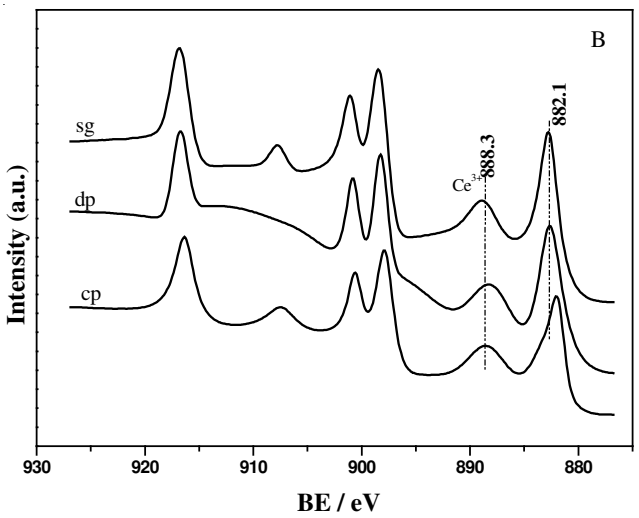

Fig. 6. XPS spectra of Ce 3d: (A) as prepared catalysts, (B) reduced samples

The X-ray photoelectron spectra of the Ce 3d binding energies of as prepared $Ce_{0.9}Cu_{0.1}O_Y$ catalysts and the reduced samples are shown in Fig. 6. As shown in Fig. 6A, the Ce3d spectrum shows six peaks at about 882.1, 888.2, 897.8, 900.3, 906.8 and 916.3 eV, which are consistent with the established characteristics of Ce(IV) 3d final state by Burroughs *et al.*[47], suggesting that the main valence of cerium in the composite was +4. Noticeably, the characteristic peaks of Ce^{3+} at *ca.* 883 and 903 eV were not obvious in the fresh or the reduced samples (Fig. 6B). Therefore, the degree of reduction of Ce^{4+} was measured using the ratio of the 916.3 eV peak area to sum of the peak areas (Table-2). The ratio for the fresh CeO_2 is 13.7 % and for the reduced catalyst is 11.0 and 10.5 and 9.9 % for fresh $Ce_{0.9}Cu_{0.1}O_Y$-cp, dp and sg, respectively, as shown in Table-2. A reduced CeO_2 surface due to the presence of copper is confirmed by a decreasing ratio and this proved the existence of the redox couple Ce^{4+}/Ce^{3+} in the $Ce_{0.9}Cu_{0.1}O_Y$ catalysts. On the other hand, no Ce_2O_3 crystallite peaks appearing on XRD pattern in Fig. 2 indicated that Ce_2O_3 content was very low. After being reduced by hydrogen at 300 ºC, the ratio differed depending on the preparation routes. The value decreased for $Ce_{0.9}Cu_{0.1}O_Y$-dp and $Ce_{0.9}Cu_{0.1}O_Y$-sg samples; however, no obvious difference was observed for $Ce_{0.9}Cu_{0.1}O_Y$-cp.

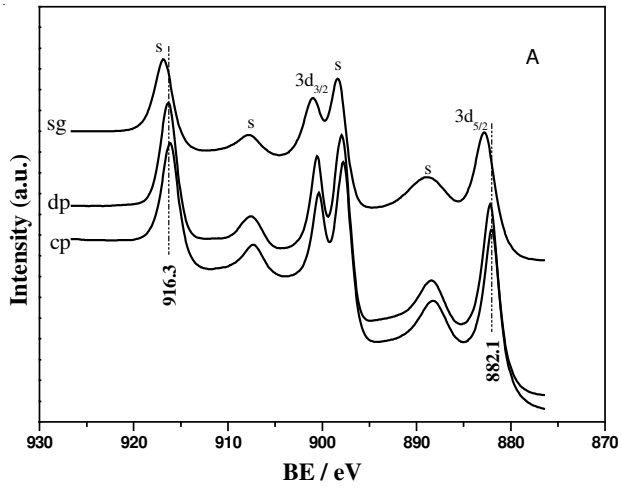

TABLE-2
OXIDATION STATES OF FRESH AND REDUCED $Ce_{0.9}Cu_{0.1}O_Y$, AS DETERMINED FROM XPS SPECTRA

Samples		$Cu2p_{3/2}$ sat.1/ Cu $2p_{3/2}$ (%)	$Ce3d_{5/2}$ CeIV/ Ce(tot) (%)
CuO		50-60	–
CeO_2		–	13.7
$Ce_{0.9}Cu_{0.1}O_{2-\delta}$-cp	Fresh	8.7	11.0
	Reduced at 300 ºC	2.6	10.9
$Ce_{0.9}Cu_{0.1}O_{2-\delta}$-dp	Fresh	13.4	10.5
	Reduced at 300 ºC	0.9	7.5
$Ce_{0.9}Cu_{0.1}O_{2-\delta}$-sg	Fresh	9.9	9.9
	Reduced at 300 ºC	3.0	8.5

The typical spectra of Cu 2p binding energies of the $Ce_{0.9}Cu_{0.1}OY$ catalyst before and after reduction are shown in Fig. 7. The peaks of Cu $2p_{3/2}$ and Cu $2p_{1/2}$ of the fresh catalysts are centered at about 932.3-932.9 and 952.1-953.0 eV, respectively. And the spectra are easily characterized by satellites appearing in the 948 eV (sat. 1) and 967 eV (sat. 2) regions. It is well known that these satellites characterize CuO, whereas they are absent with Cu_2O or metallic copper[45,46]. The reduction at 300 ºC resulted in a slight shift of the principal peak and the significant decrease of the intensity of Cu^{2+} satellite peaks. Indeed, lower binding energy for the Cu $2p_{3/2}$ peak (932.2-933.1 eV) is characteristic of Cu_2O[48], thus, the Cu 2p XPS might suggest the presence of Cu^+, in addition to Cu^{2+} species, on the $Ce_{0.9}Cu_{0.1}O_Y$ composite surface. However, the formation of the Cu^+ species is contestable; the feature might be due to either the strong interaction of the copper clusters with cerium oxide[49] or the inducement by substitution at the interface of the CuO and CeO_2 phase because of the similarity of the Ce^{4+} and Cu^+ ionic radii[50]. In addition, it is noticeable that the Cu $2p_{3/2}$ value is less convincing to distinguish between Cu_2O and Cu^0 because they are essentially identical. On the other hand, the ratio of the intensities of the satellite peaks to those of the principal peaks (noted as sat. 1/ Cu $2p_{3/2}$) as an index of the degree of reduction of copper was considered. As shown in Table-2, the intensity ratios of the nonreduced catalysts are

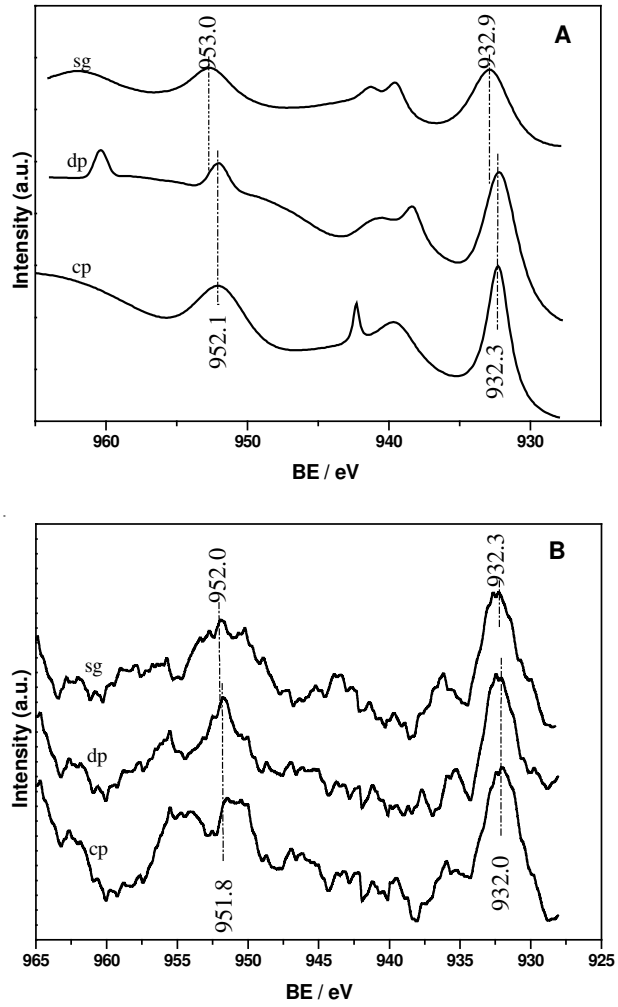

Fig. 7. XPS spectra of Cu 2p: (A) as prepared catalysts, (B) reduced samples

markedly lower than that of pure CuO. Low sat. 1/ Cu $2p_{3/2}$ values suggested that the reduced copper species was present in $Ce_{0.9}Cu_{0.1}O_Y$ composite. Though the Cu^+ and Cu^0 species can be differentiated by their different kinetic energies in the Auger Cu_{LMM} line position[51], it was not possible to identify the exact oxidation state of the reduced copper species because of the low concentration of copper species on the surface in this study[52]. In addition, it is clear that CuO is stabilized well in the $Ce_{0.9}Cu_{0.1}O_Y$-dp catalyst prepared by the deposition-precipitation method compared with the other methods. The comparison of the Cu^{2+} and Ce^{4+} species content before and after reduction leads to the conclusion that $Ce_{0.9}Cu_{0.1}O_Y$-dp catalyst showed the highest reducibility concordant with H_2-TPR results. This may have resulted from the interaction between the Ce^{4+}/Ce^{3+} and the $Cu^{2+}/Cu^{(Y)+}$ couples taking place at boundaries of nanocrystalline ceria (CeO_{2-x}). Since all three XPS measurements were performed at the same power of X-ray beam and data acquisition time, this result may give a reasonable comparison of reducibility of the copper species on different catalysts. The high reducibility of copper species is likely to be responsible for the high SRM catalytic activity of the $Ce_{0.9}Cu_{0.1}O_Y$-dp catalyst.

The identification of oxygen species on metals and oxides has attracted much attention in selective and complete oxidation reactions, since in the study of reaction mechanisms it is essential to identify the important intermediates in the reaction. It can be observed from Fig. 8 that O 1s shows in two main peaks, the one at about 530 eV is attributed to the lattice oxygen of CeO_2 and Cu_2O phases and the shoulder peak at about 532 eV is assigned to hydroxyl species on the surface and oxygen coordinated to Ce^{3+} species. After reduction, a shift in the peaks to higher binding energy was observed for all samples.

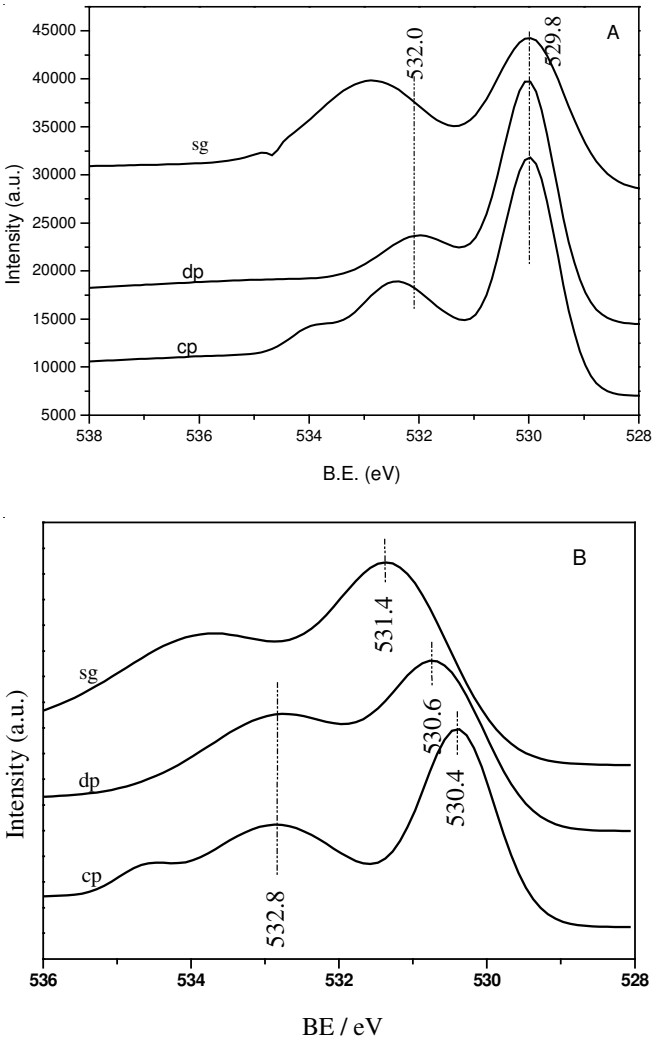

Fig. 8. XPS spectra of O 1s: (A) as prepared $Ce_{0.9}Cu_{0.1}O_Y$ catalysts, (B) reduced $Ce_{0.9}Cu_{0.1}O_Y$ samples

Steam reforming of methanol over $Ce_{0.9}Cu_{0.1}O_Y$ catalysts: The effect of reaction temperature on the catalytic performance of the $Ce_{0.9}Cu_{0.1}O_Y$ catalysts is illustrated in Fig. 9. The steam reformation of methanol experiments were conducted with steam in excess of stoichiometry (H_2O/CH_3OH = 1.5 molar ratio) to ensure the completion of methanol conversion. It is clear that the preparative method is an important factor in the performance of the catalyst in the steam reforming of methanol reaction. It can be seen that the yield of hydrogen increased with increasing reaction temperature and that the catalytic activity of all the samples was greatly increased as the temperature was raised above 260 ºC. Among the catalysts, $Ce_{0.9}Cu_{0.1}O_Y$-dp exhibits the highest methanol conversion and hydrogen production yield in the temperature range studied. When reaction temperature was higher than 260 ºC, all the

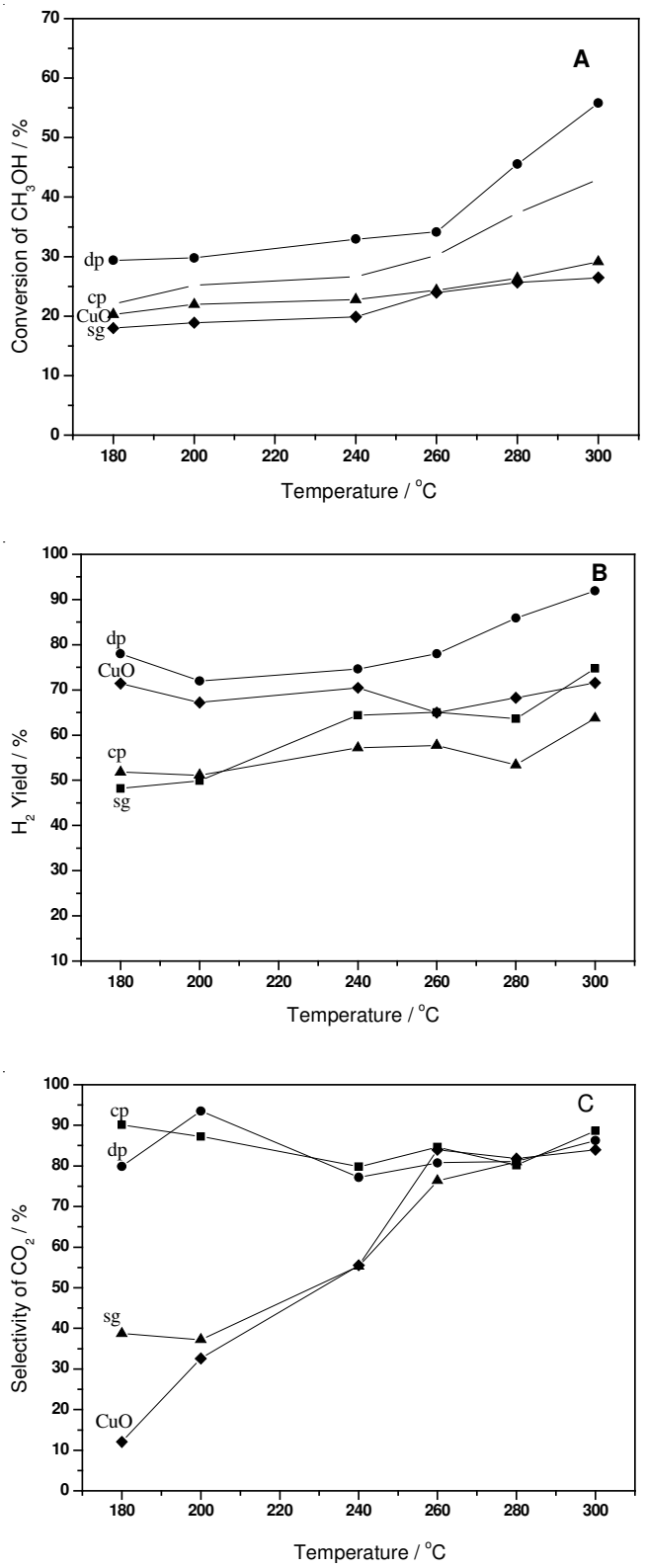

Fig. 9. Effect of reaction temperature on catalytic activity over $Ce_{0.9}Cu_{0.1}O_Y$ catalyst prepared by various methods: (A) conversion of methanol; (B) H_2 yield and (C) selectivity of CO_2

catalysts including CuO, showed increasing activity. It is apparent that, $Ce_{0.9}Cu_{0.1}O_Y$-cp and $Ce_{0.9}Cu_{0.1}O_Y$-dp catalysts gave a higher CO_2 selectivity than $Ce_{0.9}Cu_{0.1}O_Y$-sg and CuO. In addition, it is noticeable that selectivity of CO_2 slightly deceased with increasing reaction temperature for $Ce_{0.9}Cu_{0.1}O_Y$-dp and $Ce_{0.9}Cu_{0.1}O_Y$-cp. However, the opposite trend was observed for the $Ce_{0.9}Cu_{0.1}O_Y$-sg catalyst. The high selectivity for carbon dioxide shown by $Ce_{0.9}Cu_{0.1}O_Y$-dp and $Ce_{0.9}Cu_{0.1}O_Y$-cp indicates that the main reaction is steam reforming with a minor reverse water-gas shift reaction to produce carbon monoxide.

Fig. 10 shows the relationship of flow rate of methanol/water mixture with methanol conversion. It demonstrates that the catalytic activities of the catalysts are also found to be strongly dependent on the space velocity of the feeding liquid. The liquid flow rate of methanol/water is varied between 1.2 and 4.2 mL min^{-1}. It can be seen that methanol conversion increase rapidly with decreasing flow rate for all the samples. The results are consistent with previous investigations concerning the effect of space velocity or contact time on the steaming reforming of methanol[53]. In this experiment, $Ce_{0.9}Cu_{0.1}O_Y$-dp showed more activity than the other samples, further confirming the superior performance of the catalyst derived by the deposition-precipitation method. Fig. 10B indicates that no significant difference in selectivity for CO_2 was observed with the changing liquid flow rate of the methanol/water mixture.

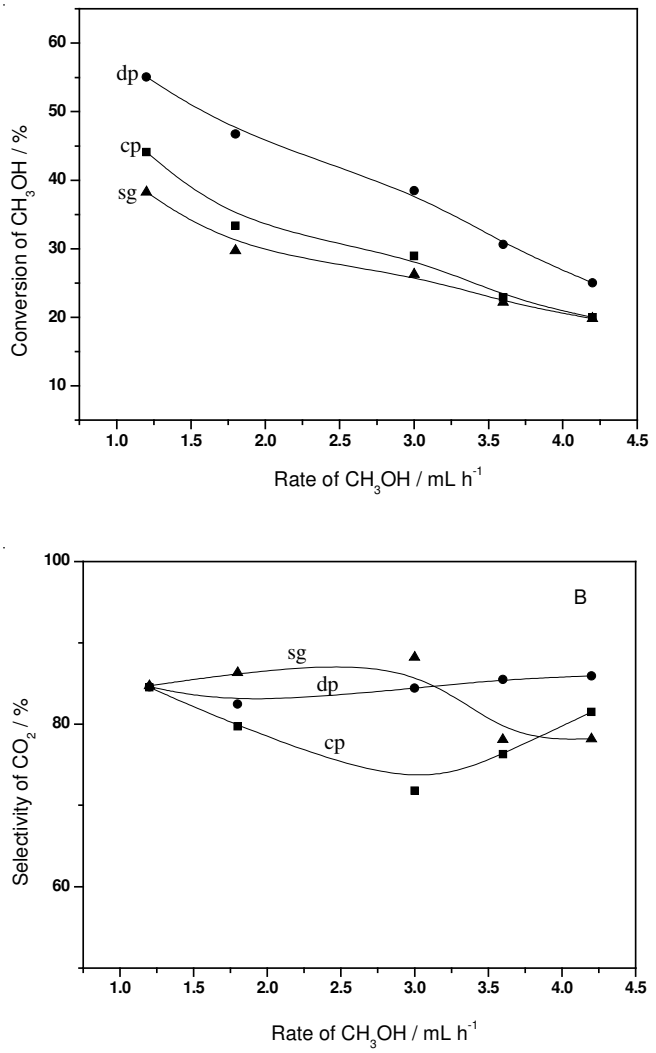

Fig. 10. Effect of liquid flow rate of methanol/water on catalytic activity over $Ce_{0.9}Cu_{0.1}O_Y$ catalysts prepared by various methods: (A) conversion of methanol and (B) selectivity of CO_2

Conclusion

In summary, several methods including deposition-precipitation, co-precipitation and sol-gel were employed for the preparation of $Ce_{0.9}Cu_{0.1}O_Y$ solid solution catalysts for methanol steam reforming. The catalytic results demonstrated that the preparative method has an important influence on the structure of the catalyst and catalytic activity for hydrogen production from the steam reforming of methanol. The characterizations indicated that a solid solution forms in the $Ce_{0.9}Cu_{0.1}O_Y$ catalyst. It is shown that deposition-precipitation method can allow the production of a $Ce_{0.9}Cu_{0.1}O_Y$ catalyst with a large surface area as well as good reducibility. It exhibits a higher catalytic activity for the steam reforming of methanol than the catalysts prepared by other methods presented and could be a promising catalyst for the production of hydrogen from methanol. Furthermore, improving the methanol conversion is been undergone in our research group.

ACKNOWLEDGEMENTS

The authors thank the financial support from the Key Research Project J51503 of Shanghai Committee of Science and Technology, Shanghai Education Committee Foundation 11YZ221 and Science Foundation YJ2012-29 of Shanghai Institute of Technology.

REFERENCES

1. D. Sperling and J.S. Cannon, The Hydrogen Energy Transition, Academic Press, Burlington (2004).
2. P.J. de Wild and M.J.F.M. Verhaak, *Catal. Today*, **60**, 3 (2000).
3. L. Ma, B. Gong, T. Tran and M.S. Wainwright, *Catal. Today*, **63**, 499 (2000).
4. C.S. Guo, S.-I. Rujita, S. Matsumoto and N. Takezawa, *J. Mol. Catal. A*, **124**, 123 (1997).
5. R. Pérez-Hernández, A. Gutiérrez-Martínez, J. Palacios, M. Vega-Hernández and V. Rodríguez-Lugo, *Int. J. Hydrogen Energy*, **36**, 6601 (2011).
6. A. Penkova, L. Bobadilla, S. Ivanova, M. I. Domínguez, F. Romero-Sarria, A.C. Roger, M.A. Centeno and J.A. Odriozola, *Appl. Catal. A*, **392**, 184 (2011).
7. R. Pérez-Hernández, A. Gutiérrez-Martínez, J. Palacios, M. Vega-Hernández and V. Rodríguez-Lugo, *Int. J. Hydrogen Energy*, **36**, 6601 (2011).
8. E.S. Ranganathan, S.K. Bej and L.T. Thompson, *Appl. Catal. A*, **289**, 153 (2005).
9. R. Pérez-Hernández, A.D. Avendano, E. Rubio and V. Rodriguez-Lugo, *Top. Catal.*, **54**, 572 (2011).
10. Y. Men, G. Kolb, R. Zapf, M. O'Connell and A. Ziogas, *Appl. Catal. A*, **380**, 15 (2010).
11. Q.-L. Zhang and R. Farrauto, *Appl. Catal. A*, **395**, 64 (2011).
12. T. Takeguchi, Y. Kani, M. Inoue and K. Eguchi, *Catal. Lett*., **83**, 49 (2002).
13. H. Purnama, F. Girgsdies, T. Ressler, J.H. Schattka, R.A. Caruso, R. schomäcker and R. Schlögl, *Catal. Lett*., **94**, 61 (2004).
14. H. Oguchi, T. Nishiguchi, T. Matsumoto, H. Kanai, K. Utani, Y. Matsumura and S. Imamura, *Appl. Catal. A*, **281**, 69 (2005).
15. P. Yaseneva, S. Pavlova, V. Sadykov, E. Moroz, E. Burgina, L. Dovlitova, V. Rogov, S. Badmaev, S. Belochapkin and J. Ross, *Catal. Today*, **138**, 175 (2008).
16. T.-J. Huang and H.-M. Chen, *Int. J. Hydrogen Energy*, **35**, 6218 (2010).
17. H. Kobayashi, N. Takazawa and M. Shimokawabe, *Stud. Surf. Sci. Catal*., **16**, 697 (1983).
18. T. Tanabe, S. Kameoka and A.-P. Tsai, *Appl. Catal. A*, **384**, 241 (2010).
19. P.P.C. Udani, P.V.D.S. Gunawardana, H.C. Lee and D.H. Kim, *Int. J. Hydrogen Energy*, **34**, 7648 (2009).
20. A. Trovarelli, *Catal. Rev*., **38**, 439 (1996).
21. P. Fornasiero, G. Balducci, R.D. Monte, J. Kaspar, V. Sergo, G. Gubitosa, A. Ferrero and M. Graziani, *J. Catal*., **164**, 173 (1996).
22. L. Fan and K. Fujimoto, *J. Catal*., **172**, 238 (1997).
23. A. Trovarelli, *Catal. Rev.-Sci. Eng*., **38**, 439 (1996).
24. L. Li, G. Li, Y. Che and W. Su, *Chem. Mater*., **12**, 2567 (2000).
25. M. Luo, J. Chen, J. Lu and Z. Feng, C. Li, *Chem. Mater*., **13**, 1491 (2001).
26. A.I. Kozlov, D.H. Kim, A. Yezerets, P. Andersen, H.H. Kung and M.C. Kung, *J. Catal*., **209**, 417 (2002).
27. W.-J. Shan, Z.-C. Feng, Z.-L. Li, J. Zhang, W.-J. Shen and C. Li, *J. Catal*., **228**, 206 (2004).
28. L.A. Ying, J. Liu, L. Mo, H. Lou and X. Zheng, *Int. J. Hydrogen Energy*, **37**, 1002 (2012).
29. X.-C. Zheng, X.-L. Zhang, X.-Y. Wang, S.-R. Wang and S.-H. Wu, *Appl. Catal. A*, **295**, 142 (2005).
30. J.-W. Park, J.-H. Jeong, W.-L. Yoon, H. Jung, H.-T. Lee, D.-K. Lee, Y.-K. Park and Y.-W. Rhee, *Appl. Catal. A*, **274**, 25 (2004).
31. J. Li, P.-F. Zhu, S.-F. Zuo, Q.-Q. Huang and R.-X. Zhou, *Appl. Catal. A*, **381**, 261 (2010).
32. Y.-Y. Liu, T. Hayakawa, K. Suzuki, S. Hamakawa, T. Tsunoda, T. Ishii and M. Kumagai, *Appl. Catal. A*, **223**, 137 (2002).
33. A.K. Sinha and K. Suzuki, *J. Phys. Chem. B*, **109**, 1708 (2005).
34. Y. Brik, M. Kacimi, B.V. Francois and M. Ziyad, *J. Catal*., **211**, 470 (2002).
35. X.-L. Tang, B.-C. Zhang, Y. Li, Y.-D. Xu, Q. Xin and W.-J. Shen, *Appl. Catal. A*, **288**, 116 (2005).
36. N. Uekawa, M. Ueta, Y.-J. Wu and K. Kakegawa, *Chem. Lett*., **31**, 854 (2002).
37. G. Avgouropoulos and T. Ioannides, *Appl. Catal. A*, **244**, 155 (2003).
38. M. Kobayashi and M. Flytzani-Stephanopoulos, *Ind. Eng. Chem. Res*., **41**, 3115 (2002).
39. S.-M. Zhang, W.-P. Huang, X.-H, Qiu, B.-Q. Li, X.-C. Zheng and S.-H. Wu, *Catal. Lett*., **80**, 41 (2002).
40. P. Bera, K.R. Priolkar, P.R. Sarode, M.S. Hegde, S. Emura, R. Kumashiro and N.P. Lalla, *Chem. Mater*., **14**, 3591 (2002).
41. B.M. Reddy, A. Khan, Y. Yamada, T. Kobayashi, S. Loridant and J.-C. Volta, *Phys. Chem. B*, **107**, 11475 (2003).
42. J.E. Spanier, R.D. Robinson, F. Zhang, S.-W. Chan and I.P. Herman, *Phys. Rev. B*, **64**, 245407 (2001).
43. G.R. Rao, H.R. Sanjan and B.G. Mishra, *Colloids Surf. A*, **220**, 261 (2003).
44. P. Ratnasamy, D. Srinivas, C.V.V. Satyanarayana, P. Manikandan, R. R.S. Kumaran, M. Sachin and V.N. Shetti, *J. Catal*., **221**, 455 (2004).
45. X. Wang, J.A. Rodriguez, J.C. Hanson, D. Gamarra, A. Martinezzrias and M. Fernandez-Garcia, *J. Phys. Chem. B*, **109**, 19595 (2005).
46. M.F. Luo, Y.P. Song, J.Q. Lu, X.Y. Wang and Z.Y. Pu, *J. Phys. Chem. C*, **111**, 12686 (2007).
47. P. Burroughs, A. Hamnett, A. F. Orchard and G. Thonton, *J. Chem. Soc. Dalton Trans*, 1686 (1976).
48. G. Avgouropoulos, T. Ioannides and H. Matralis, *Appl. Catal. B*, **56**, 87 (2005).
49. W. Liu and M. Flytzani-Stehanopoulos, *J. Catal*., **153**, 304 (1995).
50. S. Hocevar, U.L. Krasovec, B. Orel, A.S. Arico and H. Kim, *Appl. Catal. B*, **28**, 113 (2000).
51. P.H. Matter, D.J. Braden and U.S. Ozka, *J. Catal*., **223**, 340 (2004).
52. Y. Men, H. Gnaser, R. Zapf, V. Hessel, C. Ziegler and G. Kolb, *Appl. Catal. A*, **277**, 83 (2004).
53. J. Agrell, H. Birgersson and M. Boutonnet, *J. Power Sources*, **106**, 249 (2002).